NIH Public Access
Author Manuscript
Apoptosis. Author manuscript; available in PMC 2015 May 01.

Published in final edited form as:
Apoptosis. 2014 May ; 19(5): 776–788. doi:10.1007/s10495-014-0974-3.

LR-90 prevents methylglyoxal-induced oxidative stress and apoptosis in human endothelial cells

James L. Figarola, **Jyotsana Singhal**, **Samuel Rahbar**, **Sanjay Awasthi**, and **Sharad S. Singhal**

Departments of Diabetes and Metabolic Diseases Research, Beckman Research Institute of the City of Hope National, Medical Center, NCI Designated Comprehensive Cancer Center, Gonda North, RM # 2108, 1500 E. Duarte Rd, Duarte, CA 91010, USA

Sharad S. Singhal: ssinghal@coh.org

Abstract

Methylglyoxal (MGO) is a highly reactive dicarbonyl compound known to induce cellular injury and cytoxicity, including apoptosis in vascular cells. Vascular endothelial cell apoptosis has been implicated in the pathophysiology and progression of atherosclerosis. We investigated whether the advanced glycation end-product inhibitor LR-90 could prevent MGO-induced apoptosis in human umbilical vascular endothelial cells (HUVECs). HUVECs were pre-treated with LR-90 and then stimulated with MGO. Cell morphology, cytotoxicity and apoptosis were evaluated by light microscopy, MTT assay, and Annexin V-FITC and propidium iodide double staining, respectively. Levels of Bax, Bcl-2, cytochrome c, mitogen-activated protein kinases (MAPKs) and caspase activities were assessed by Western blotting. Reactive oxygen species (ROS) generation and mitochondrial membrane potential (MMP) were measured with fluorescent probes. LR-90 dose-dependently prevented MGO-associated HUVEC cytotoxicity and apoptotic biochemical changes such as loss of MMP, increased Bax/Bcl-2 protein ratio, mitochondrial cytochrome c release and activation of caspase-3 and 9. Additionally, LR-90 blocked intracellular ROS formation and MAPK (p44/p42, p38, JNK) activation, though the latter seem to be not directly involved in MGO-induced HUVEC apoptosis. LR-90 prevents MGO-induced HUVEC apoptosis by inhibiting ROS and associated mitochondrial-dependent apoptotic signaling cascades, suggesting that LR-90 possess cytoprotective ability which could be beneficial in prevention of diabetic related-atherosclerosis.

Keywords

Apoptosis; Atherosclerosis; Diabetes; Glycation; Methylglyoxal; Oxidative stress

© Springer Science+Business Media New York 2014

Correspondence to: Sharad S. Singhal, ssinghal@coh.org.

Conflict of interest The authors declare that they have no conflict of interest.

NIH-PA Author Manuscript
NIH-PA Author Manuscript
NIH-PA Author Manuscript

NIH-PA Author Manuscript
NIH-PA Author Manuscript
NIH-PA Author Manuscript

Introduction

Methylglyoxal (MGO) is a physiological metabolite formed by the fragmentation of triose phosphates, which are intermediates of glycolysis [1, 2]. MGO is also formed by lipid peroxidation, in the catabolism of threonine, and in the oxidation of acetone [2, 3]. Additionally, MGO is present ubiquitously in beverages and foods, as well as cigarette smoke [4]. A recent study revealed that the plasma MGO level is significantly increased in diabetic patients [5]. MGO reacts with arginine or lysine residues of proteins and forms advanced glycation end products (AGEs) such as imidazolones (MG-H1, MG-H2, MG-H3), N^{ε}-carboxyethyllysine (CEL), methylglyoxal-lysine dimer (MOLD), argpyrimidine, tetrahydropyrimidine (THP), and 2-ammonio-6-({2-[4-ammonio-5-oxido-5-oxopently)amino]-4-methyl-4,5-dihydro-1H-imidazol-5-ylidene}amino) hexanoate (MODIC) (4). MGO and MGO-derived AGEs have been implicated in the pathophysiology of diabetic complications [6, 7] and hypertension [8].

Endothelial cells (ECs) that form the inner lining of all blood vessels may be subject to stress that can perturb cellular components involved in intracellular signaling transduction pathway, resulting in cell proliferation or death. Apoptosis, or programmed cell death, has emerged as a key element in the complex pathophysiology underlying the development and progression of atherosclerosis [9]. Apoptotic ECs have been detected on luminal surface of atherosclerotic coronary vessels but not in normal vessels, suggesting a link between EC apoptosis and the pathology of atherosclerosis [10]. Moreover, EC apoptosis has been shown to promote platelet adhesion [11], as well as vessel thrombosis and EC denudation, two major features of plaque erosion [12]. Apoptotic EC could also cause myocardial damage not only via rupture of atherosclerotic lesions, but also due to pro-apoptotic effects on cardio-myocyte [13] and direct induction of over-proliferation of nearby smooth muscle cells [14]. Thus, EC apoptosis may represent a form of injury that may compromise vessel wall permeability to cytokines, growth factors, lipids and immune cells, increase coagulation, and down-regulation of vasohomeostatic regulators such as nitric oxide [9].

Previous studies have shown that MGO can induce apoptosis in human vascular ECs [15–17], and that this cytotoxic effect occurs mainly through induction of reactive oxygen species (ROS) [15, 17–19], although the molecular mechanism underlying this process is not yet fully understood. The aim of this study was to examine whether LR-90, an AGE inhibitor with pleiotropic properties (antioxidant, anti-inflammatory, carbonyl scavenger) [20–23] could exert a cytoprotective effect on the endothelium by inhibiting apoptosis induced by MGO, and to investigate its effects on the various signaling pathways associated with apoptosis, including oxidative stress, MAPK and caspase activation, and mitochondrial-dependent cell death signaling pathways.

Materials and methods

Chemicals and antibodies

MTT [3-(4,5-dimethylthiazol-2-yl)-2,5-diphenyltetrazolium bromide] kit was purchased from Millipore (Billerica, MA). Dihydroethidium (DHE), 5-(and-6)-chloromethyl-2′, 7-dichlorodihydrofluorescein diacetate (CM-H_2DCFDA or DCF), and 3, 3,

NIH-PA Author Manuscript

NIH-PA Author Manuscript

NIH-PA Author Manuscript

dihexyloxacarbocyanine iodide (DiOC6(3)), were obtained from Invitrogen (Carlsbad, CA). Antibodies against caspase-3, caspase-9, p38 MAPK, p44/p42 MAPK, Bcl-2, Bax, cytochrome c and β-actin were purchased from Cell Signaling Technology (Beverly, MA). Anti-JNK antibodies were from R&D Systems, Inc. (Minneapolis, MN). MAPK inhibitors SB 239063, PD 98059, SP 600125 were from EMD Chemicals Inc. (Gibbstown, NJ). LR-90 (Fig. 1a) was synthesized by Dr. Christopher Lincoln at the Chemical GMP Synthesis Facility, Translational Medicinal Chemistry Laboratory, Beckman Research Institute of the City of Hope. The purity of the compound was confirmed by ^{1}H-NMR, ^{13}C-NMR and HRMS-ESI analyses. Unless otherwise stated, all other chemicals and reagents of analytical grade were purchased from Sigma–Aldrich (St. Louis, MO).

Cell culture

HUVECs were obtained from Cascade Biologics (Portland, OR). Cells were cultured in Medium 200 (Cascade Biologics) supplemented with 10 % fetal bovine serum (FBS), streptomycin (100 mg/ml) and penicillin (100 units/ml). HUVECs were maintained in 5 % CO_2 at 37 °C. Cells at passages 4–8 were used for all experiments.

Cell viability and morphological examination

HUVECs were plated into 96-well micro-titer plates at a density of 1×10^5 cells/well. After 18 h, cells were pre-treated with indicated concentrations of test compounds for 1 h and then co-cultured with MGO (0–0.4 mM) for 24 h. After incubation, cell viability was determined using the colorimetric MTT assay kit following the manufacturer's instructions. HUVEC morphological changes were observed under light microscope (AX70, Olympus, Tokyo, Japan) equipped with a digital camera (Retiga EXi, QImaging, Surrey, BC, Canada).

Assessment of apoptosis

To determine the effects of LR-90 on apoptosis/necrosis induced by MGO in HUVECs, the FITC Annexin V-FITC/ PI double staining of cells was evaluated using the FITC Annexin V Apoptosis Detection Kit (BD Biosciences, San Diego, CA). Briefly, cells (5×10^5) were seeded onto 6-well plate and incubated for 24 h at 37 °C in culture medium containing the testing agents at the indicated final concentrations. After incubation, cells were washed with PBS, trypsinized, and resuspended in calcium-enriched HEPES buffer. Cells were stained for 15 min with Annexin V-FITC and propidium iodide (PI), and then analyzed by flow cytometry (CyAn ADP9, Beckman Coulter, Fullerton, CA). Approximately 5×10^4 counts were made for each sample. The percentage distribution of normal (viable), early apoptotic, late apoptotic and necrotic cells was calculated using Summit software (version 4.2, Cytomation Inc., Fort Collins, CO).

Protein extraction and Western blotting

HUVECs were pre-treated with test compounds and incubated with MGO at indicated time points (1, 2, 4 h). Total cytosolic proteins were extracted with Triton-based lysis buffer (Epitomics, Burlingame, CA) and protein concentration was determined using DC Protein Assay kit (Bio-Rad, Hercules, CA). Equal amounts of proteins (~50 μg) were loaded onto 10–20 % Criterion gels (Bio-Rad), separated by gel electrophoresis, and then transferred to

NIH-PA Author Manuscript

NIH-PA Author Manuscript

NIH-PA Author Manuscript

nitrocellulose membranes. Membranes were blocked with 5 % skimmed milk in Tris-buffered saline containing 0.05 % Tween 20 (TBS-T) before incubation for overnight at 4 °C with primary antibody (1:1000 dilution) against phospho-p38, phospho-p44/p42, phospho-JNK, cytochrome c, caspase-3, caspase-9, Bcl-2 or Bax proteins. Immuno-reactive proteins were visualized by peroxidase-labeled secondary antibodies and ECL system (Western Lightning Chemiluminescence Reagent, Perkin-Elmer, MA). Equal loading of proteins was confirmed by stripping and re-probing the membranes with β-actin, total p38 MAPK, p44/p42 MAPK or JNK antibodies. Band intensities were quantified using a densitometer and analyzed by Quantity One software (Bio-Rad).

Detection and measurement of intracellular ROS

Intracellular ROS generation was assessed using CM-H_2-DCFDA, a cell-permeant probe that is hydrolyzed by intracellular esterases to DCFH. In the presence of hydrogen peroxide or low molecular weight peroxides produced by the cells, DCFH is oxidized to form highly fluorescent DCF, and the fluorescent intensity is proportional to the amount of peroxide produced in the cells. DHE staining was also used to evaluate superoxide generation. In the presence of superoxide anion, DHE is oxidized to ethidium bromide, which binds to DNA. Briefly, cells were plated in a 12-well plate in complete medium 200 plus 2 % FBS. After 24 h, cells were pre-treated with or without test compounds for 15 min, followed by co-incubation with MGO for 45 min. Adherent cells were then washed with warm RPMI 1640 without phenol red media and CM-H_2-DCFDA (20 μM) or DHE (10 μM) was added for 30 min and incubated at 37 °C. Cells were then rinsed twice with PBS, and fluorescence intensity was monitored and photographed on an Olympus IX81 inverted microscope. Photographs were taken adjusting the same exposure time and gain detector in order to diminish the photobleaching of the fluorescent dyes. Fluorescent intensity for each image was quantified using ImagePro Premiere software (Media Cybernetics, Inc., Rockville, MD).

Measurement of mitochondrial membrane potential **(MMP, Δψm)—**Mitochondrial membrane potential was determined with $DiOC_6(3)$ staining. $DiOC_6(3)$ is cationic fluorescent dye that is incorporated into the mitochondria in an Δψm -dependent manner. Briefly, HUVECs (2×10^5) were seeded overnight into 24-well black plates, and pre-treated with and without test compounds for 30 min. MGO (0.4 mM) was added to each well for 2 h. Cells were then rinsed with the medium, incubated with 50 nm $DiOC_6(3)$ for 20 min at 37 °C, and the overall fluorescence intensity of each treatment was measured with a fluorescent plate reader (excitation 485 nm; emission 535 nm). In addition, the concentration of retained $DiOC_6(3)$ in 25,000 cells of each sample was measured using flow cytometry. $DiOC_6(3)$ was excited at 488 nm, and fluorescence was analyzed at 525 nm (FL-1) after logarithmic amplification.

Cytochrome c release assay

HUVECs (1×10^7) were treated with MGO with and without test compounds for 3 h, harvested, washed twice with ice-cold PBS (pH 7.4), and the cytosolic and mitochondrial fractions were then isolated using Cytochrome c Release Apoptosis Assay Kit (Calbiochem, La Jolla, CA) according to the manufacturer's protocol. The resultant cytosolic fractions

NIH-PA Author Manuscript

NIH-PA Author Manuscript

NIH-PA Author Manuscript

were resolved on SDS-PAGE and the level of cytochrome *c* was visualized by Western blotting.

Data analyses

Statistical analyses were performed using GraphPad Prism 6 (GraphPad Software, Inc., San Diego, CA). Data are presented as means ± SEM. Statistical evaluations were performed using one-way ANOVA followed by post hoc multiple group comparisons using Bonferroni test. A P value <0.05 was considered statistically significant.

Results

LR-90 prevents MGO-induced cytotoxicity and apoptosis

LR-90 was synthesized by the Drug Discovery Core Facility within City of Hope's Comprehensive Cancer Center. The structure of LR-90 is represented in Fig. 1a. We first examined the visual morphological changes of HUVECs after treatment with various concentrations of MGO under light microscopy. As shown in Fig. 1b, MGO treatment for 24 h induced a cytotoxic morphological change (apparent reduction in cell density and loss of confluency, cell shrinkage into rounder shape, as well as increase in number of bright objects representing floating cell fragments) in a dose-dependent manner. These morphological changes were associated with decreased cell viability as assessed by the MTT assay, with ~ 40 % cell death at 0.4 mM MGO concentration (Fig. 1c). Pre-treatment with LR-90 (10–100 μM) resulted in a dose-dependent prevented MGO-induced cell death (Fig. 1b, c). Cells treated with LR-90 alone up to 100 μM had no effect on cell viability (data not shown).

To examine whether this MGO-induced cell death is associated with apoptosis, flow cytometry of annexin V-FITC and PI double staining was performed. Treatment of cells with MGO (0.4 mM) for 24 h significantly increased the number of apoptotic and necrotic cells relative to untreated control (Fig. 2a, b). The enhanced apoptosis and necrosis were significantly suppressed by LR-90, particularly at 100 μM concentrations. Similar anti-apoptotic effects were observed with cells treated with the AGE inhibitor/carbonyl scavenger aminoguanidine (AG) (Fig. 1 and 2) and the antioxidant N-acetyl cysteine (NAC).

LR-90 prevents MGO-induced alterations in mitochondrial membrane permeability

During the process of apoptosis, the mitochondrial trans-membrane potential (Δψm) decreases. This results from the opening of the permeability transition pore (PTP) which causes local disruption of the outer mitochondrial membrane and release of pro-apoptotic factors [24]. To test whether inhibition of mitochondrial function disruption was involved in the anti-apoptotic effects of LR-90, we used the fluorescent cationic probe $DiOC_6(3)$. Viable cells have a high mitochondrial membrane potential (Δψm) and display bright $DiOC_6(3)$ fluorescence, while apoptotic cells display dull $DiOC_6(3)$ fluorescence and lower Δψm due to the depolarization and disruption of the mitochondrial membrane. MGO treatment of cells significant reduced the overall DiOC6(3) fluorescent intensity compared with control cells, indicating that the Δψm of the mitochondria was depolarized (Fig. 3a). This was further supported by flow cytometry analyses, where the fluorescence signal shifted to the left for

NIH-PA Author Manuscript

NIH-PA Author Manuscript

NIH-PA Author Manuscript

MGO-treated HUVECs, demonstrating that fewer cells retained DiOC6(3) in their mitochondria (Fig. 3b). Pretreatment with LR-90 prevented the loss in Δψm as indicated by higher fluorescence readings and marked reversion of the shift of the fluorescent signal to the right similar to control with increasing concentrations of LR-90. Similarly, pre-incubation with AG (2 mM) or NAC (2 mM) also prevented the loss of Δψm (Fig. 3a, b), suggesting that both carbonyl scavenger and antioxidant treatments can block MGO-induced mitochondrial membrane dysfunction in HUVECs.

Because studies have shown that outer mitochondrial membrane permeability is regulated by the activities of the Bcl-2 family of pro-apoptotic and anti-apoptotic proteins for initiating apoptosis [25], we investigated by Western blotting whether MGO-induced apoptosis was associated with changes in the expression of anti-apoptotic Bcl-2 and pro-apoptotic Bax proteins in HUVECs. It is well-established that the ratio between Bcl-2 and Bax proteins is an important factor in the regulation of apoptosis rather than the level of each protein separately. An increase of Bax/Bcl-2 ratio is sufficient to promote apoptosis in mammalian cells and induce cell death by directly activating the mitochondrial apoptotic pathway [25]. As shown in Fig. 4a, stimulation of cells with MGO caused a marked reduction in Bcl-2 protein expression and a significant increase in Bax protein expression as compared with untreated control. Treatment with LR-90 dose-dependently decreased the expression of Bax protein, while increasing the expression of Bcl-2 protein, thus attenuating the increase in Bax/Bcl-2 ratio, with the maximal effect seen at 100 μM concentration (Fig. 4a). Similar effects were observed when cells were pre-treated with AG or NAC, indicating again that both carbonyl scavenger and antioxidant can both regulate the expression of Bcl-2 family proteins in MGO-induced apoptosis.

LR-90 inhibits the release of cytochrome c and prevented caspase activation

The disruption of the mitochondrial membrane function is known to result in the release of the mitochondrial enzyme cytochrome c into the cytosol [26]. As detected using Western blot analyses, stimulation of cells with MGO resulted in almost 2.5-fold increase in the levels of cytochrome c in the cytosol compared with untreated control cells. Pre-incubation with LR-90 dose-dependently inhibited this MGO-induced cytochrome *c* release into the cytosol (Fig. 4b).

To further investigate downstream apoptotic signaling during MGO-induced cell death, we analyzed the activation of caspase-3 and caspase-9, hallmark apoptotic execution enzymes, by Western blotting. MGO treatment of HUVECs markedly stimulated the activation of both caspases. Pre-incubation with LR-90 clearly inhibited caspase-3 and caspase-9 activation, with 100 μM of LR-90 showing almost undetected caspase-3 and caspase-9 activities similar with untreated cells. Treatment with NAC or AG also prevented cytochrome c release and activation of both caspases (Fig. 4b).

LR-90 suppresses MGO-induced intracellular ROS generation

Elevated amounts of intracellular ROS may induce apoptosis by themselves or act as intracellular messengers during the cell death induced by various other kinds of stimuli [27]. To examine whether increased oxidative stress is associated with MGO-induced apoptosis in

NIH-PA Author Manuscript

NIH-PA Author Manuscript

NIH-PA Author Manuscript

HUVECs, we measured both hydrogen peroxide and superoxide generation using CM-H_2DCFDA (DCF) and DHE staining, respectively. As shown in Fig. 5, both hydrogen peroxide (DCF in green) and superoxide (DHE in red) were significantly increased in HUVECs exposed to MGO. Treatment with LR-90 dose-dependently suppressed ROS production in these cells with 100 μM of LR-90 almost completely abolished ROS production. Similar antioxidant effects were seen with AG and NAC treatments (Fig. 5).

LR-90 inhibits MGO-stimulated MAPK activation

Studies in several cell lines have also shown that MAPK activation is an important signal mechanism associated with MGO-induced apoptosis. Using specific antibodies and Western blot analyses, we observed that 1 h treatment of cells with MGO induced activation of p38, p44/p42 and JNK. Pre-treatment with LR-90 blocked the activation of all three MAPKs similarly as observed with AG and NAC (Fig. 6a). However, pharmacological inhibition of MAPK pathways using specific MAPK inhibitors, SB 239063 (p38), PD98059 (p44/42), SP600125 (JNK), failed to protect cells from MGO-induced cell death (Fig. 6a, b, c).

Discussion

MGO is a highly reactive carbonyl compound known to induce cellular injury and cytoxicity. In this study, we examined the effects of LR-90 on MGO-induced apoptosis in HUVECs. LR-90 is an AGE inhibitor [21, 22] that has protective effects against nephropathy [20], retinopathy [28], and atherosclerosis [29] in experimental diabetes. It also exhibits anti-inflammatory effects on monocytes activated by S100b or TNF-α [23]. Our present data from morphological observations, MTT assay and Annexin V-FITC/PI double staining clearly indicated that MGO is a potent inducer of cytotoxicity and apoptosis in HUVECs, and that LR-90 protected cells from apparent cell death in a dose-dependent manner. Consistent with these observations, pretreatment with LR-90 prevented the release of cytochrome c from the mitochondria into the cytosol, inhibited both caspase-3 and caspase-9 activation, and attenuated the increase in Bax/Bcl-2 ratio, thus confirming the cytoprotective properties of LR-90 against MGO-induced apoptosis. Additionally, we found that LR-90 prevented MGO-induced loss of $\Delta\psi m$, an early event in the apoptosis pathway. Based on these results, it is likely that MGO induces mitochondrial-dependent apoptosis in HUVECs. Interestingly, we observed similar cytoprotective effects in HUVECs that were pre-incubated with the antioxidant NAC, indicating that mitochondrial membrane dysfunction and subsequent apoptosis maybe downstream events associated with the increase of ROS.

It was previously reported that MGO-induced cytotoxicity in ECs is also associated with activation of MAPK signaling, including JNK, p38, and p44/p42 [30]. We confirmed in our present study that all three MAPKs were activated by MGO. Treatment with LR-90 dose-dependently inhibited the activation of all three MAPKs. These results showed that LR-90 could modulate the MAPK signaling pathways in MGO-treated HUVECs. However, we observed that pharmacological inhibition of p38 MAPK, p44/42 MAPK, and JNK using specific inhibitors SB239063, PD98059, SP600125, respectively, failed to suppress MGO-induced HUVEC apoptosis. These findings indicate that the MAPK pathways are not

NIH-PA Author Manuscript

NIH-PA Author Manuscript

NIH-PA Author Manuscript

directly involve in MGO-associated apoptosis in HUVECs, and their activation may be just a consequence of upstream activators/signal molecules such as intracellular ROS production. Indeed, previous studies demonstrated that treatment with antioxidants prevented MAPK activation in MGO-treated cells [31, 32].

To further clarify the upstream signal molecules affected by LR-90 in MGO-induced apoptosis, we then investigated its effects on ROS generation. There are several ways by which intracellular ROS levels could be increased by MGO. These include production of superoxide anion and hydrogen peroxide during the glycation reaction of amino acids or proteins, depletion of the glutathione content of cells during MGO metabolism by the glyoxalase system, and inactivation of enzymes which scavenge ROS such as superoxide dismutases, glutathione peroxidases, and glutathione transferases [33–35]. More importantly, MGO-stimulated increase in ROS levels can also contribute to the vicious cycle of ROS-AGE-RAGE-ROS formation in the vasculature [36]. Experiments with human aortic ECs suggested that MGO stimulates superoxide anion production primarily through the mitochondrial pathway [37]. Using the fluorescent probes DCF and DHE, we also detected high levels of hydrogen peroxide and superoxide formation when HUVECs were stimulated prior to the time point (within 1 h) that apoptotic cell death became evident. Our results are in agreement with previous studies showing ROS generation as an important upstream signal molecule in MGO-induced apoptosis [17, 18, 31, 32]. In our experiments, both AGE inhibitors LR-90 and AG suppressed ROS formation and associated mitochondrial-dependent cell death signaling pathway. These two compounds have been known to scavenge free radicals in a cell-free environment [21, 22]. Recently, we also have shown that LR-90 inhibited intracellular superoxide formation in activated monocytes via modulation of the $gp91^{phox}$ subunit (NOX2) [23], as well as ROS production from human aortic ECs stimulated with high glucose and/or saturated fatty acids [38]. Taken together, these data strongly suggest that the ability of LR-90 to inhibit ROS production plays a significant protective role in MGO-induced apoptosis. Interestingly, antioxidants such as NAC and phenolic acids have also been shown to prevent MGO-induced apoptosis [39]. Indeed, we observed that NAC blocked MGO-induced apoptosis via inhibition of ROS production, decreased Bax-Bcl-2 ratio, prevention of $\Delta\psi m$ collapse and cytochrome c release, and subsequent attenuation of caspase activation. Thus, the current findings strongly suggest that intracellular ROS generation triggered by MGO can be blocked by LR-90 and other antioxidants such as NAC and AG, and support the hypothesis that LR-90 inhibits MGO-induced apoptotic biochemical changes by blocking ROS formation.

In addition to their antioxidant properties, both LR-90 and AG are known to trap/scavenge carbonyl compounds like MGO [21, 22, 40]. Therefore, it is logical to assume that this scavenging activity could also influence the amount of intracellular MGO that reacts with cellular components and triggers the apoptosis pathway. Interestingly, similar anti-apoptotic effects in MGO-treated human aortic ECs were observed with metformin, another known carbonyl scavenger [41]. Whether this MGO-scavenging/ neutralizing property occurs outside or inside the cells is uncertain, particularly with exogenously applied MGO used in these experiments. A recent study has reported increased mitochondrial MGO content, leading to CEL formation and increased mitochondrial ROS production, after cells were treated with exogenous MGO [42]. Moreover, incubation of cultured rat aortic ECs and

NIH-PA Author Manuscript

NIH-PA Author Manuscript

NIH-PA Author Manuscript

HUVECs with MGO significantly increased intracellular MGO levels in these cells, which was prevented by co-incubation with AG or NAC [43]. Whether MGO-derived intracellular AGE formation leads directly to cytotoxicity and apoptosis remains unclear. Further investigations how LR-90 might affect intracellular MGO levels, MGO-protein adduct formation, mitochondrial ROS generation, as well as intracellular antioxidant enzymes, should provide additional mechanistic insights into the cytoprotective effects of LR-90 on MGO-associated apoptosis.

It has been suggested that the initiation of atherosclerosis is closely linked to endothelial dysfunction [9]. Although there is currently no direct evidence that MGO is the main cause of diabetes-related atherosclerosis in humans, MGO has been implicated to play a major role in vascular damage to endothelial cells and in the development of vascular disease. For instance, chronic feeding of MGO in rats promoted oxidative stress, endothelial dysfunction and inflammation concomitant with increased MGO-derived N^{ε}-carboxyethyl-lysine (CEL) and RAGE expression in the aorta [44]. Moreover, higher levels of protein-bound MGO-derived AGEs such as 5-hydro-5-methylimidazolone (MG-H1) and tetrahydropyrimidine (THP) were found in human atherosclerotic plaques that are highly associated with apoptosis and inflammatory markers [45, 46]. A recent genome wide gene expression profile studies in HUVECs showed that MGO treatment may cause cytotoxicity and tissue injury in the human endothelium by altering genes involved in apoptosis, cell cycle, cell adhesion and inflammatory responses [47]. Thus, the ability of LR-90 to prevent MGO-induced oxidative stress and apoptosis in vascular ECs may be protective against development of diabetic atherosclerosis. Indeed, our preliminary studies showed that LR-90 prevented the progression of diabetes-accelerated atherosclerosis in diabetic apolipoprotein E knockout mice [29].

The MGO concentrations and shorter incubation times used in our study may represent a likely difference to in vivo conditions, where the endothelium would be expected to be exposed to a continual external flux of MGO over an extended time period. MGO plasma levels are estimated to be about 0.3–0.9 μM in healthy individuals and can increase to 1.5–3.3 μM in diabetic patients [48]. However, others demonstrated that plasma methylglyoxal concentration in poorly controlled human diabetic patients can go as high as 400 μM [5]. The intracellular MGO level is likely much higher than the plasma MGO level in the diabetic condition because diabetic tissues are chronically exposed to high MGO levels, which can cause marked intracellular MGO accumulation. It should also be noted that the reported plasma levels reflect steady-state concentrations (i.e. residual material that has not reacted with plasma components), rather than the total concentration to which proteins are likely to be exposed to over their biological lifetime. Indeed, MGO levels in rat tissues (particularly in the aorta) are an order of magnitude higher than in plasma as detected by solid phase extraction and quantification by electrospray ionization liquid chromatography mass spectrometry [49]. Additionally, it is reported that only a small percentage of exogenous MGO is incorporated into cultured cells [50], although it is not clear how MGO moves across cellular membranes. In the present studies, we used 50–400 μM of MGO, and this concentration caused cell injury and apoptosis to HUVECs in a concentration-dependent manner. Similar MGO concentration ranges have been used by a number of investigators for

NIH-PA Author Manuscript

NIH-PA Author Manuscript

NIH-PA Author Manuscript

studying MGO-induced apoptosis and other biochemical changes in ECs and other types of human cells [15, 16, 27, 30–32, 37, 39, 41, 42, 47].

Conclusions

Present studies indicated that LR-90 prevented MGO-induced HUVEC cytotoxicity and apoptosis via inhibition of oxidative stress and associated downstream signaling apoptotic cascades, including loss of Δψm, cytochrome c release and caspase activation. Since ECs morphological change and apoptosis are early steps of atherosclerosis, our results suggest that LR-90 might be protective against diabetes-related atherosclerosis.

Acknowledgments

This work was supported by the National Institutes of Health Grant (CA 77495). The authors are grateful to Jacquelin and Isaac Moradi for their many years of support and research funding. Funding from Department's Chair (Prof. Arthur Riggs) and Beckman Research Institute of the City of Hope is also acknowledged. We are also thankful to Dr. Brian Armstrong (Microscope Core, City of Hope) and Lucy Brown (Analytical Core, City of Hope) for their technical assistance in microscopy and flow cytometry analyses, respectively.

Abbreviations

AG	Aminoguanidine
AGE	Advanced glycation end-product
Ecs	Endothelial cells
HUVECs	Human umbilical vascular endothelial cells
LR-90	Methylene bis [4,4′-(2 chlorophenylureido phenoxyisobutyric acid)]
MAPKs	Mitogen-activated protein kinases
MGO	Methylglyoxal
MMP	Mitochondrial membrane potential
NAC	N-acetyl cysteine
ROS	Reactive oxygen species

References

1. Phillips SA, Thornalley PJ. The formation of methylglyoxal from triose phosphates. Investigation using a specific assay for methylglyoxal. Eur J Biochem. 1993; 212:101–105. [PubMed: 8444148]
2. Thornalley PJ. Pharmacology of methylglyoxal: formation, modification of proteins and nucleic acids, and enzymatic detoxification–a role in pathogenesis and anti-proliferative chemotherapy. Gen Pharmacol. 1996; 27:565–573. [PubMed: 8853285]
3. Kalapos MP. Methylglyoxal in living organisms: chemistry, biochemistry, toxicology and biological implications. Toxicol Lett. 1999; 110:145–175. [PubMed: 10597025]
4. Nemet I, Varga-Defterdarovic L, Turk Z. Methylglyoxal in food and living organisms. Mol Nutr Food Res. 2006; 50:1105–1117. [PubMed: 17103372]
5. Lapolla A, Flamini R, Dalla Vedova A, Senesi A, Reitano R, Fedele D, Basso E, Seraglia R, Traldi P. Glyoxal and methylglyoxal levels in diabetic patients: quantitative determination by a new GC/MS method. Clin Chem Lab Med. 2003; 41:1166–1173. [PubMed: 14598866]

NIH-PA Author Manuscript

NIH-PA Author Manuscript

NIH-PA Author Manuscript

6. Vander Jagt DL. Methylglyoxal, diabetes mellitus and diabetic complications. Drug Metab Drug Interact. 2008; 23:93–124.
7. Fosmark DS, Torjesen PA, Kilhovd BK, Berg TJ, Sandvik L, Hanssen KF, Agardh CD, Agardh E. Increased serum levels of the specific advanced glycation end product methylglyoxal-derived hydroimidazolone are associated with retinopathy in patients with type 2 diabetes mellitus. Metabolism. 2006; 55:232–236. [PubMed: 16423631]
8. Wang X, Desai K, Chang T, Wu L. Vascular methylglyoxal metabolism and the development of hypertension. J Hypertension. 2005; 23:1565–1573.
9. Choy JC, Granville DJ, Hunt DW, McManus BM. Endothelial cell apoptosis: biochemical characteristics and potential implications for atherosclerosis. J Mol Cell Cardiol. 2001; 33:1673–1690. [PubMed: 11549346]
10. Alvarez RJ, Gips SJ, Moldovan N, Wilhide CC, Milliken EE, Hoang AT, Hruban RH, Silverman HS, Dang CV, Goldschmidt-Clermont PJ. 17-betaestradiol inhibits apoptosis of endothelial cells. Biochem Biophys Res Commun. 1997; 237:372–381. [PubMed: 9268719]
11. Bombeli T, Schwartz BR, Harlan JM. Endothelial cells undergoing apoptosis become proadhesive for non-activated platelets. Blood. 1999; 93:3831–3838. [PubMed: 10339490]
12. Durand E, Scoazec A, Lafont A, Boddaert J, Al Hajzen A, Addad F, Mirshahi M, Desnos M, Tedgui A, Mallat Z. In vivo induction of endothelial apoptosis leads to vessel thrombosis and endothelial denudation: a clue to the understanding of the mechanisms of thrombotic plaque erosion. Circulation. 2004; 109:2503–2506. [PubMed: 15148270]
13. Scarabelli T, Stephanou A, Rayment N, Pasini E, Comini L, Curello S, Ferrari R, Knight R, Latchman D. Apoptosis of endothelial cells precedes myocyte apoptosis in ischemia/reperfusion injury. Circulation. 2001; 104:253–256. [PubMed: 11457740]
14. Qin C, Liu Z. In atherogenesis, the apoptosis of endothelial cell itself could directly induce over-proliferation of smooth muscle cells. Med Hypotheses. 2007; 68:275–277. [PubMed: 17011140]
15. Takahashi K, Tatsunami R, Tampo Y. Methylglyoxal-induced apoptosis of endothelial cells. Yakugaku Zasshi. 2008; 128:1443–1448. [PubMed: 18827464]
16. Baden T, Yamawaki H, Saito K, Mukohda M, Okada M, Hara Y. Telmisartan inhibits methylglyoxal-mediated cell death in human vascular endothelium. Biochem Biophys Res Commun. 2008; 373:253–257. [PubMed: 18565324]
17. Phalitakul S, Okada M, Hara Y, Yamawaki H. Vaspin prevents methylglyoxal-induced apoptosis in human vascular endothelial cells by inhibiting reactive oxygen species generation. Acta Physiol (Oxf). 2013; 209:212–219. [PubMed: 23782902]
18. Kim K, Son JW, Lee JA, Oh YS, Shinn SH. Methylglyoxal induces apoptosis mediated by reactive oxygen species in bovine retinal pericytes. J Korean Med Sci. 2004; 19:95–100. [PubMed: 14966349]
19. Desai KM, Wu L. Free radical generation by methylglyoxal in tissues. Drug Metab Drug Interact. 2008; 23:151–173.
20. Figarola JL, Scott S, Loera S, Tessler C, Chu P, Weiss L, Hardy J, Rahbar S. LR-90 a new advanced glycation endproduct inhibitor prevents progression of diabetic nephropathy in streptozotocin-diabetic rats. Diabetologia. 2003; 46:1140–1152. [PubMed: 12845431]
21. Rahbar S, Figarola JL. Novel inhibitors of advanced glycation endproducts. Arch Biochem Biophys. 2003; 419:63–79. [PubMed: 14568010]
22. Rahbar S. Novel inhibitors of glycation and AGE formation. Cell Biochem Biophys. 2007; 48:147–157. [PubMed: 17709884]
23. Figarola JL, Shanmugam N, Natarajan R, Rahbar S. Anti-inflammatory effects of the advanced glycation end product inhibitor LR-90 in human monocytes. Diabetes. 2007; 56:647–655. [PubMed: 17327432]
24. Ly JD, Grubb DR, Lawen. The mitochondrial membrane potential (delta psi(m)) in apoptosis: an update. Apoptosis. 2003; 8:115–128. [PubMed: 12766472]
25. Brunelle JK, Letai A. Control of mitochondrial apoptosis by the Bcl-2 family. J Cell Sci. 2009; 122:437–441. [PubMed: 19193868]

NIH-PA Author Manuscript

NIH-PA Author Manuscript

NIH-PA Author Manuscript

26. Gottlieb E, Armour SM, Harris MH, Thompson CB. Mitochondrial membrane potential regulates matrix configuration and cytochrome c release during apoptosis. Cell Death Differ. 2003; 10:709–717. [PubMed: 12761579]
27. Circu ML, Aw TY. Reactive oxygen species, cellular redox systems, and apoptosis. Free Radic Biol Med. 2010; 48:749–762. [PubMed: 20045723]
28. Bhatwadekar A, Glenn JV, Figarola JL, Scott S, Gardiner TA, Rahbar S, Stitt AW. A new advanced glycation inhibitor, LR-90, prevents experimental diabetic retinopathy in rats. Br J Ophthalmol. 2008; 92:545–547. [PubMed: 18211931]
29. Watson, A.; Thomas, MC.; Koh, P.; Figarola, JL.; Rahbar, S.; Jandeleit-Dahm, K. Attenuation of diabetes-associated atherosclerosis with LR-90, a novel inhibitor of AGE formation. In: Thomas, MC.; Forbes, J., editors. The Maillard Reaction: Interface between Aging. Nutrition and Metabolism: RCS Publishing; 2010. p. 137-143.
30. Yamawaki H, Saito K, Okada M, Hara Y. Methylglyoxal mediates vascular inflammation via JNK and p38 in human endothelial cells. Am J Physiol Cell Physiol. 2008; 295:C1510–C1517. [PubMed: 18842828]
31. Akhand AA, Hossain K, Mitsui H, Kato M, Miyata T, Inagi R, Du J, Takeda K, Kawamoto Y, Suzuki H, Kurokawa K, Nakashima I. Glyoxal and methylglyoxal trigger distinct signals for map family kinases and caspase activation in human endothelial cells. Free Radic Biol Med. 2001; 31:20–30. [PubMed: 11425486]
32. Fukunaga M, Miyata S, Higo S, Hamada Y, Ueyama S, Kasuga M. Methylglyoxal induces apoptosis through oxidative stress-mediated activation of p38 mitogen-activated protein kinase in rat Schwann cells. Ann N Y Acad Sci. 2005; 1043:151–157. [PubMed: 16037234]
33. Yim HS, Kang SO, Hah YC, Chock PB, Yim MB. Free radicals generated during the glycation reaction of amino acids by methylglyoxal. J Biol Chem. 1995; 270:28228–28233. [PubMed: 7499318]
34. Choudhary D, Chandra D, Kale RK. Influence of methylglyoxal on antioxidant enzymes and oxidative damage. Toxicol Lett. 1997; 93:141–152. [PubMed: 9486950]
35. Kang JH. Modification and inactivation of human Cu, Zn-superoxide dismutase by methylglyoxal. Mol Cells. 2003; 15:194–199. [PubMed: 12803482]
36. Yan SF, Ramasamy R, Schmidt AM. The RAGE axis: a fundamental mechanism signaling danger to the vulnerable vasculature. Circ Res. 2010; 106:842–853. [PubMed: 20299674]
37. Miyazawa N, Abe M, Souma T, Tanemoto M, Abe T, Nakayama M, Ito S. Methylglyoxal augments intracellular oxidative stress in human aortic endothelial cells. Free Radic Res. 2010; 44:101–107. [PubMed: 19886746]
38. Stentz FB, Kitabchi AE, Razavi L, Rahbar S. Inhibition of oxidative stress, TNF-alpha and IL 6 in human aortic endothelial cells by a novel advanced glycation end-product inhibitor, LR-90. Diabetes. 2009; 58(Suppl. 1):A205.
39. Huang SM, Chuang HC, Wu CH, Yen GC. Cytoprotective effects of phenolic acids on methylglyoxal-induced apoptosis in Neuro-2A cells. Mol Nutr Food Res. 2008; 52:940–949. [PubMed: 18481334]
40. Lo TW, Selwood T, Thornalley PJ. The reaction of methylglyoxal with aminoguanidine under physiological conditions and prevention of methylglyoxal binding to plasma proteins. Biochem Pharmacol. 1994; 48:1865–1870. [PubMed: 7986197]
41. Ota K, Nakamura J, Li W, Kozakae M, Watarai A, Nakamura N, Yasuda Y, Nakashima E, Naruse K, Watabe K, Kato K, Oiso Y, Hamada Y. Metformin prevents methylglyoxal-induced apoptosis of mouse Schwann cells. Biochem Biophys Res Commun. 2007; 357:270–375. [PubMed: 17418096]
42. Huang SM, Hsu CL, Chuang HC, Shih PH, Wu CH, Yen GC. Inhibitory effect of vanillic acid on methylglyoxal-mediated glycation in apoptotic Neuro-2A cells. Neurotoxicology. 2008; 29:1016–1022. [PubMed: 18706441]
43. Dhar A, Dhar I, Desai KM, Wu L. Methylglyoxal scavengers attenuate endothelial dysfunction induced by methylglyoxal and high concentrations of glucose. Br J Pharmacol. 2010; 161:1843–1856. [PubMed: 20825408]

NIH-PA Author Manuscript

NIH-PA Author Manuscript

NIH-PA Author Manuscript

44. Sena CM, Matafome P, Crisóstomo J, Rodrigues L, Fernandes R, Pereira P, Seica RM. Methylglyoxal promotes oxidative stress and endothelial dysfunction. Pharmacol Res. 2012; 65:497–506. [PubMed: 22425979]

45. Hanssen NM, Wouters K, Huijberts MS, Gijbels MJ, Sluimer JC, Scheijen JL, Heeneman S, Biessen EA, Daemen MJ, Brownlee M, de Kleijn DP, Stehouwer CD, Pasterkamp G, Schalkwijk CG. Higher levels of advanced glycation endproducts in human carotid atherosclerotic plaques are associated with a rupture-prone phenotype. Eur Heart J. 2013 Oct 14. 2013 in-press.

46. van Eupen MG, Schram MT, Colhoun HM, Hanssen NM, Niessen HW, Tarnow L, Parving HH, Rossing P, Stehouwer CD, Schalkwijk CG. The methylglyoxal-derived AGE tetrahydropyrimidine is increased in plasma of individuals with type 1 diabetes mellitus and in atherosclerotic lesions and is associated with sVCAM-1. Diabetologia. 2013; 56:1845–1855. [PubMed: 23620061]

47. Lee SE, Yahg H, Jeong SI, Jin Y, Park C, Park YS. Methylglyoxal-mediated alteration of gene expression in human endothelial cells. BioChip J. 2010; 5:220–228.

48. Mirza MA, Kandhro AJ, Memon SQ, Khuhawar MY, Arain R. Determination of glyoxal and methylglyoxal in the serum of diabetic patients by MEKC using stilbenediamine as derivatizing reagent. Electrophoresis. 2007; 28:3940–3947. [PubMed: 17924366]

49. Randell EW, Vasdev S, Gill V. Measurement of methyl-glyoxal in rat tissues by electrospray ionization mass spectrometry and liquid chromatography. J Pharmacol Toxicol Methods. 2005; 51:153–157. [PubMed: 15767209]

50. Che W, Asahi M, Takahashi M, Kaneto H, Okado A, Higashiyama S, Taniguchi N. Selective induction of heparin-binding epidermal growth factor-like growth factor by methylglyoxal and 3-deoxyglucosone in rat aortic smooth muscle cells: the involvement of reactive oxygen species formation and a possible implication for atherogenesis in diabetes. J Biol Chem. 1997; 272:18453–18459. [PubMed: 9218489]

NIH-PA Author Manuscript

NIH-PA Author Manuscript

NIH-PA Author Manuscript

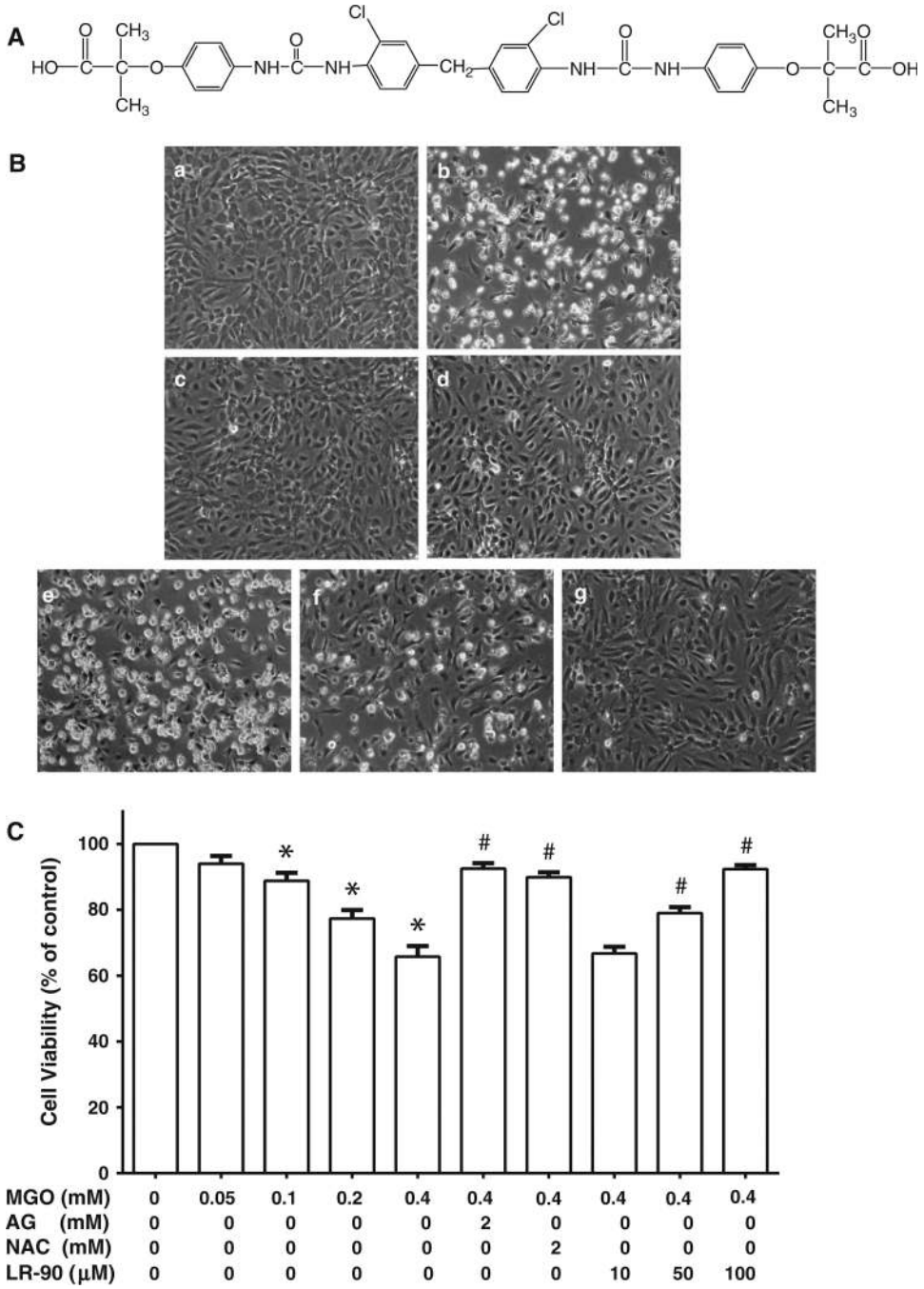

Fig. 1.

Effects of LR-90 on MGO-induced cell death in HUVECs **a** Chemical structure of LR-90, methylene bis 4,4′-(2-chloropheny-lureidophenoxyisobutyric acid). **b** Representative phase contrast photomicrographs of MGO-treated cells with and without test compounds. HUVECs were treated for 24 h with *a* 0.1 % DMSO (vehicle control); *b* MGO (0.4 mM); *c* MGO + 2 mM AG; *d* MGO + 2 mM NAC; *e–g* MGO + 10, 50, or 100 μM LR-90, respectively. Original magnification: 160x. **c** Percentage of viable cells analyzed by MTT assay after 24 h exposure to MGO in the presence of various concentrations of test

compounds. Data on graph were from three independent experiments ($n = 9$) and were analyzed by ANOVA followed by Bonferroni's post hoc test (*$p < 0.05$ *vs*. vehicle control and # $p < 0.05$ *vs*. 0.4 mM MGO treatment only)

NIH-PA Author Manuscript
NIH-PA Author Manuscript
NIH-PA Author Manuscript

NIH-PA Author Manuscript
NIH-PA Author Manuscript
NIH-PA Author Manuscript

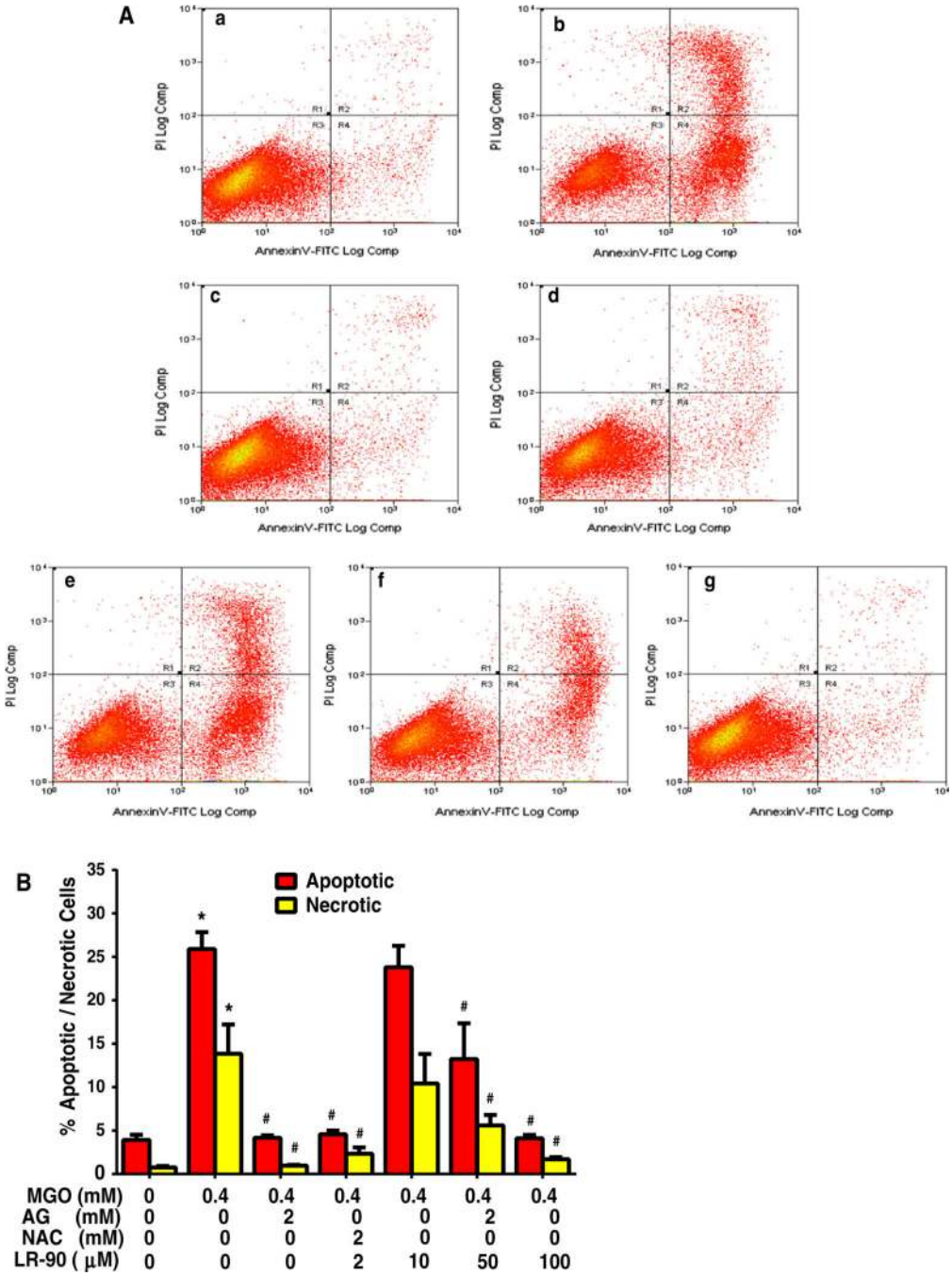

Fig. 2.

Flow cytometry analyses on the effect of LR-90 on MGO-induced apoptosis in HUVECs **a** Representative cytograms of Annexin V-FITC binding and PI uptake of MGO-stimulated HUVECs. Cells were pretreated with test compounds for 1 h then co-incubated with 0.4 mM MGO. After 24 h, cells were harvested and analyzed by flow cytometry. R1 = PI positive cells (necrotic); R2 = annexin V-FITC positive and PI positive cells (late apoptotic/ necrotic); R3 = annexin V-FITC negative and PI negative cells (normal viable cells); R4 = annexin V-FITC-positive and PI-negative cells (early apoptosis), *a* vehicle control, *b* MGO,

NIH-PA Author Manuscript

NIH-PA Author Manuscript

NIH-PA Author Manuscript

c MGO + AG (2 mM), *d* MGO + NAC (2 mM), *e* MGO + LR-90 (10 μM), *f* MGO + LR-90 (50 μM), *g* MGO + LR-90 (100 μM). **b** Mean percentage of cells in early apoptosis or late apoptosis/necrosis as analyzed by flow cytometry. Data on graph were from three independent experiments ($n = 6$) and were analyzed by ANOVA followed by Bonferroni's post hoc test (*$p < 0.05$ *vs*. vehicle control and # $p < 0.05$ *vs*. 0.4 mM MGO treatment only)

NIH-PA Author Manuscript

NIH-PA Author Manuscript

NIH-PA Author Manuscript

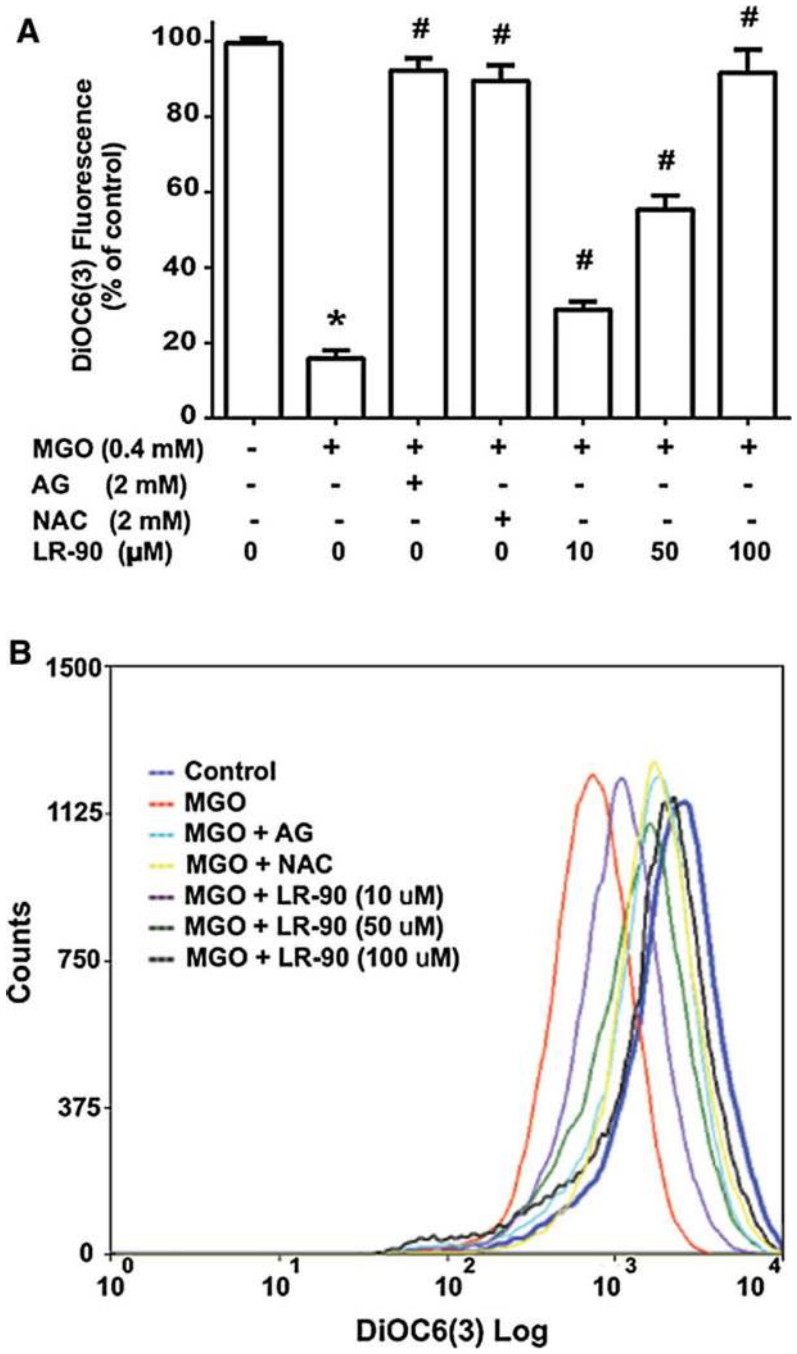

Fig. 3.

Effects of LR-90 on MGO-induced mitochondrial membrane permeability HUVECs were pre-treated with test compounds for 1 h, followed by incubation with MGO (0.4 mM) for 1 h. Cells were then rinsed and stained with the cationic fluorescent dye DiOC6(3) and then the overall fluorescence **a** was measured with a fluorescent plate reader (excitation 485 nm; emission 535 nm) or **b** analyzed by flow cytometry (excitation 488 nm; emission 525 nm). Data on graph **a** were from two independent experiments ($n = 6$) and were analyzed by

ANOVA followed by Bonferroni's post hoc test (*$p < 0.05$ *vs*. vehicle control and # $p < 0.05$ *vs*. 0.4 mM MGO treatment only)

NIH-PA Author Manuscript

NIH-PA Author Manuscript

NIH-PA Author Manuscript

NIH-PA Author Manuscript

NIH-PA Author Manuscript

NIH-PA Author Manuscript

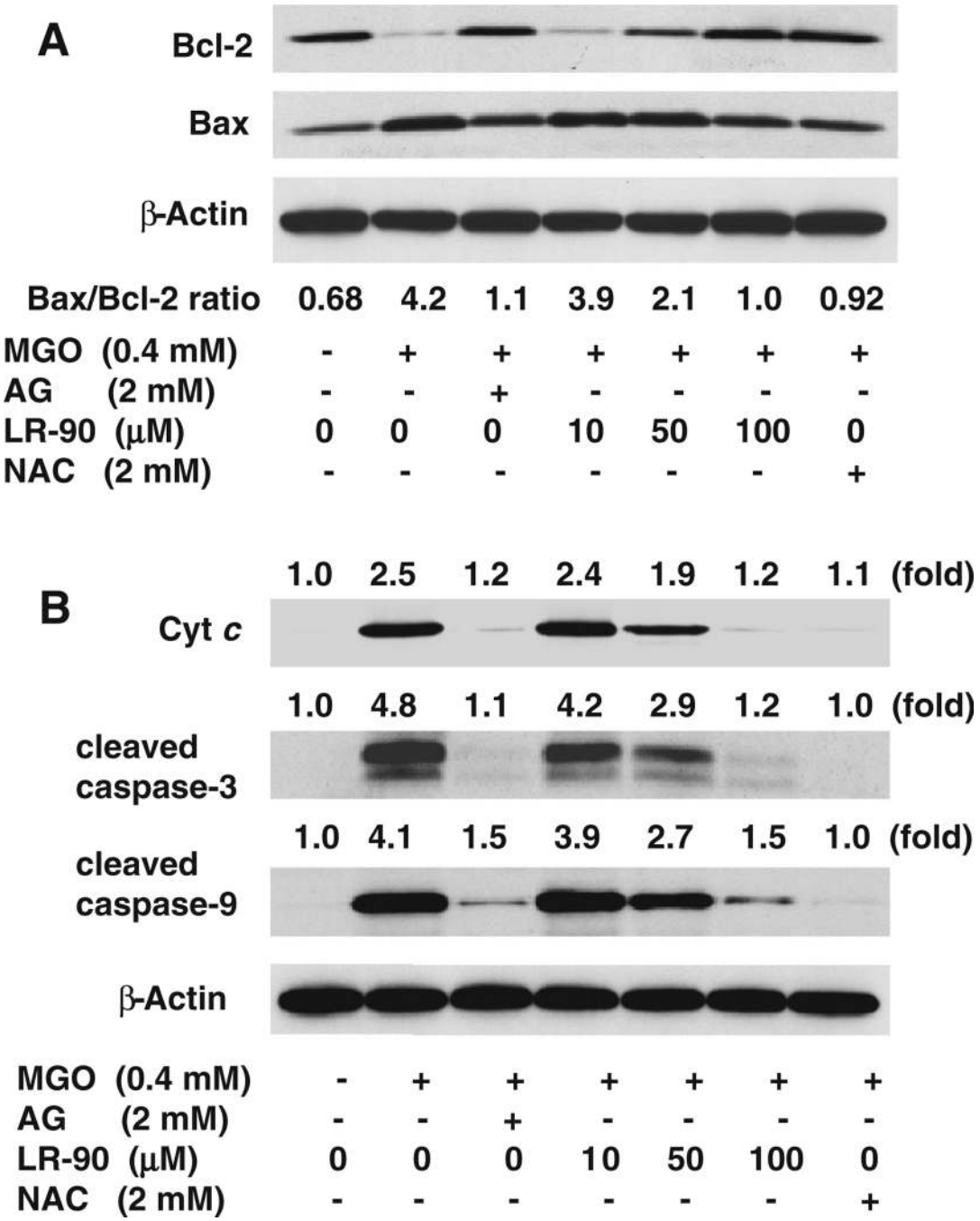

Fig. 4.

Effects of LR-90 on Bax and Bcl-2 protein expression, cytochrome c release and caspase activation in MGO-treated HUVECs **a** Representative Western blot of total cell lysates immuno-blotted and probed with antibodies against Bcl-2 (26 kDa) and Bax (20 kDa) proteins. Cells were pre-treated with test compounds for 1 h, followed by incubation with MGO (0.4 mM) for 3 h. Bax/Bcl-2 ratio quantified by densitometry and calculated with reference to β-actin protein (45 kDa). **b** Representative Western blots of cytochrome *c* (14 kDa), cleaved caspase-3 (19 and 17 kDa) and cleaved caspase-9 (37 kDa) protein

NIH-PA Author Manuscript

NIH-PA Author Manuscript

NIH-PA Author Manuscript

expression. Cells were pretreated with test compounds for 1 h, followed by incubation with MGO (0.4 mM) for 3 h. Numbers above each blot represent fold increase in protein expression relative to the control as quantified by densitometry and calculated with reference to β-actin

NIH-PA Author Manuscript

NIH-PA Author Manuscript

NIH-PA Author Manuscript

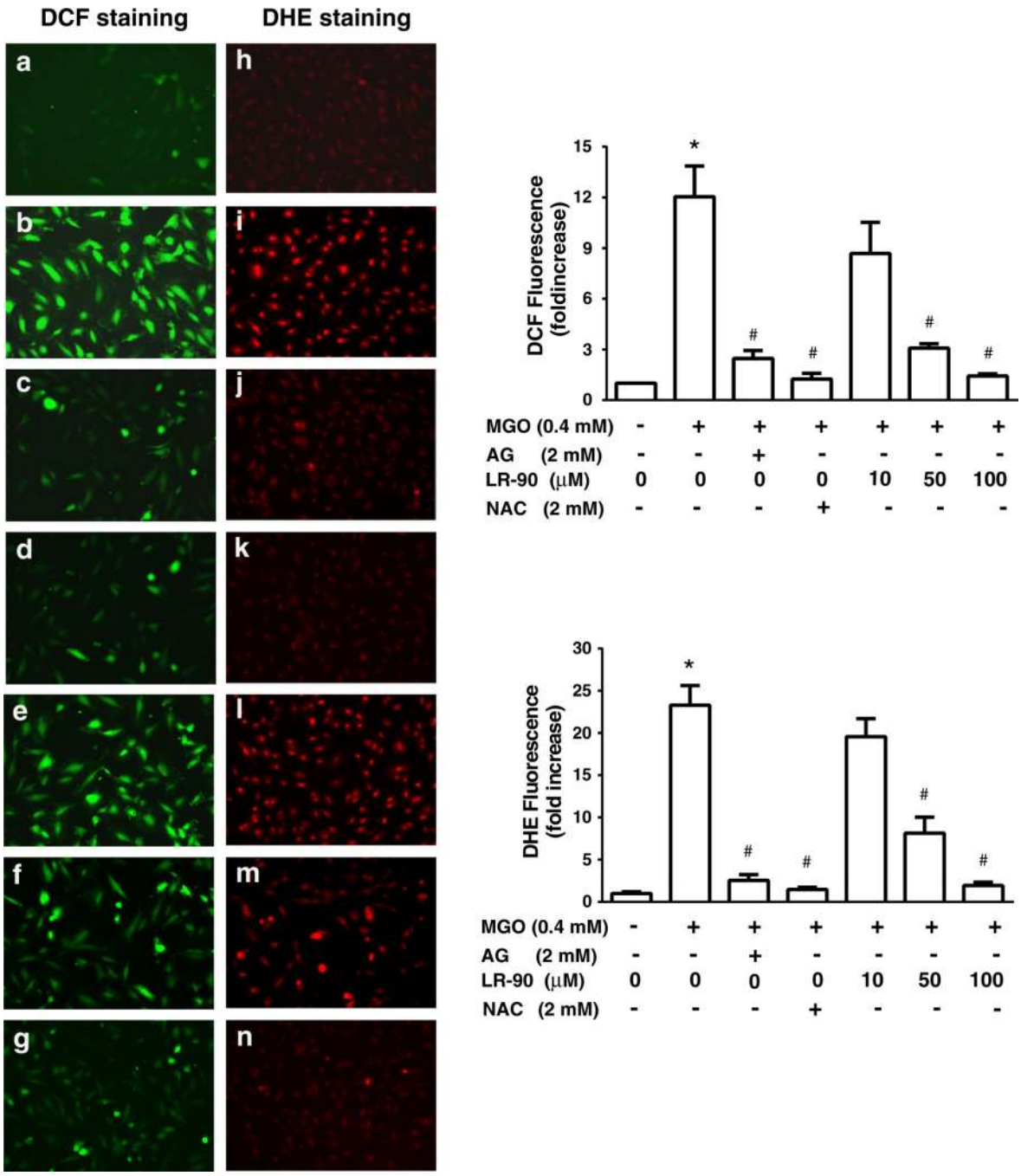

Fig. 5.

Effects of LR-90 on MGO-induced ROS generation HUVECs were pre-treated with LR-90 for 15 min followed by co-incubation with MGO (0.4 mM) for 45 min. *Green* and *red* fluorescence from DCF (**a–g**) and DHE (**h–n**) stainings, respectively, were monitored by fluorescence microscopy. **a, h** vehicle control; **b, i** MGO-treated; **c, j** MGO + AG (2 mM); **d, k** MGO + NAC (2 mM); **e, l** MGO + LR-90 (10 μM); **f, m** MGO + LR-90 (50 μM), **g, n** MGO + LR-90 (100 μM). Original magnification: 200x. Quantitative measurements of fluorescent intensity were performed using Image Pro Premiere software. Results represent

fold increase of ROS generation over control and are expressed as mean ± SEM from three independent experiments ($n = 6$). Data analyzed by ANOVA followed by Bonferroni's post hoc test (*$p < 0.05$ *vs*. vehicle control and # $p < 0.05$ *vs*. 0.4 mM MGO treatment only)

NIH-PA Author Manuscript
NIH-PA Author Manuscript
NIH-PA Author Manuscript

NIH-PA Author Manuscript

NIH-PA Author Manuscript

NIH-PA Author Manuscript

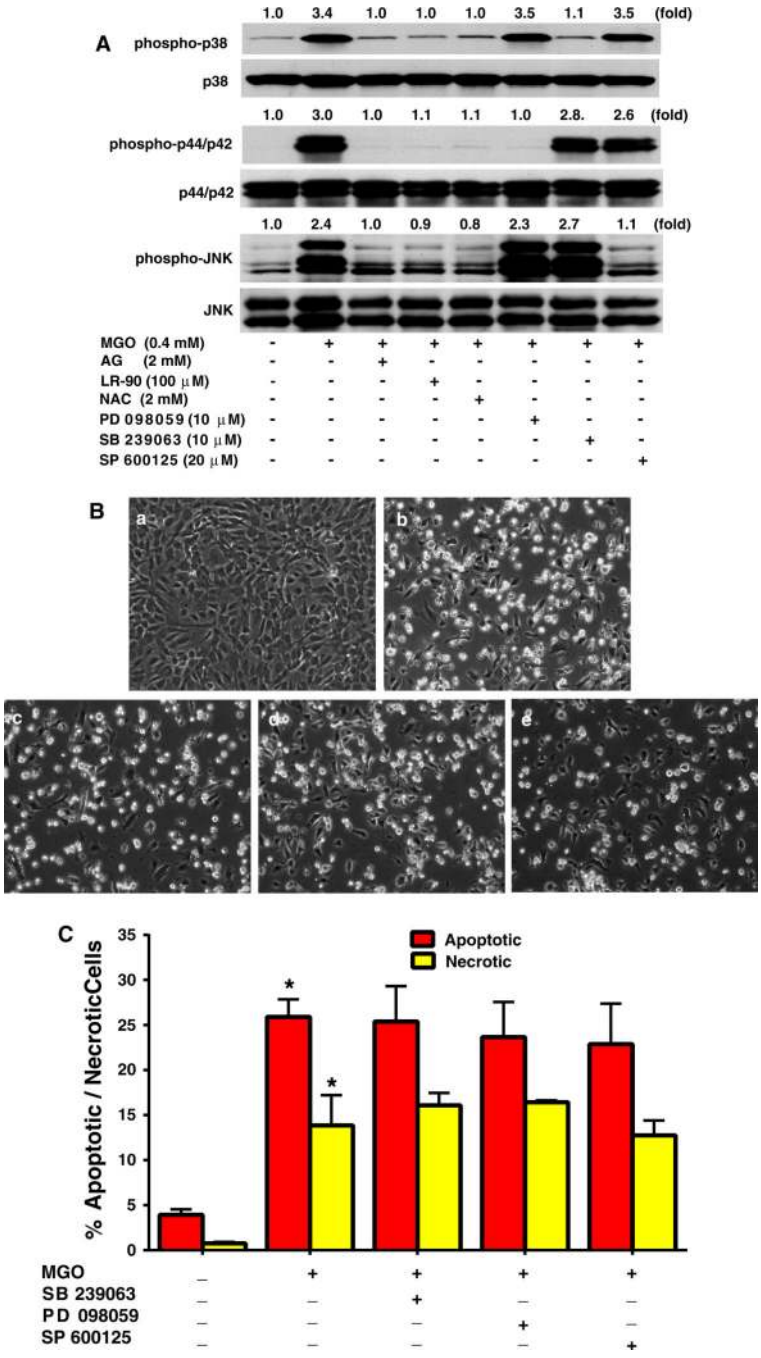

Fig. 6.

Effects of LR-90, AG and NAC on MAPK signaling pathways in HUVECs **a** Effects of LR-90 on MAPK signaling pathways. Representative Western blots of total and phosphorylated forms of MAPKs. Cells were pre-treated with test compounds for 1 h, and then stimulated with 0.4 mM MGO for 1 h. Numbers above each blot represent fold increase in protein expression of phosphorylated MAPKS relative to the control as quantified by densitometry and calculated with reference to the total forms of each MAPK. **b** Representative phase contrast photomicrographs of MGO-treated HUVECs with MAPK

NIH-PA Author Manuscript

NIH-PA Author Manuscript

NIH-PA Author Manuscript

inhibitors. Cells were pretreated with test compounds for 1 h then co-incubated with *a* vehicle control; *b* MGO (0.4 mM); *c* MGO + 10 μM SB 239063; *d* MGO + 10 μM PD 98059; *e* MGO + 20 μM SP 600125, for 24 h. **c** Mean percentage of cells in early apoptosis or late apoptosis/necrosis as analyzed by flow cytometry. Data on graph were from three independent experiments ($n = 6$) and were analyzed by ANOVA followed by Bonferroni's post hoc test (*$p < 0.05$ *vs*. vehicle control)